Chapter 5

Lattice Quantum Chromodynamics

C. T. Sachrajda

School of Physics and Astronomy,
University of Southampton, Southampton SO17 1BJ, UK
cts@soton.ac.uk

I review the the application of the lattice formulation of QCD and large-scale numerical simulations to the evaluation of non-perturbative hadronic effects in Standard Model Phenomenology. I present an introduction to the elements of the calculations and discuss the limitations both in the range of quantities which can be studied and in the precision of the results. I focus particularly on the extraction of the QCD parameters, i.e. the quark masses and the strong coupling constant, and on important quantities in flavour physics. Lattice QCD is playing a central role in quantifying the hadronic effects necessary for the development of precision flavour physics and its use in exploring the limits of the Standard Model and in searches for inconsistencies which would signal the presence of new physics.

1. Introduction

Quantum Chromodynamics (QCD) is now well established as the theory of the strong nuclear force. This has been possible largely as a result of the property of *asymptotic freedom* which states that the force between quarks and gluons becomes weak at distances much less than 1 fm. At such short distances, the standard analytical tool of perturbation theory can be applied and the results compared with experimental results as discussed, e.g. in the chapter by R. K. Ellis in this Book.[1] However at the typical hadronic scale of about 1 fm, the strong coupling constant α_s is too large for perturbation theory to be applied and *non-perturbative* methods are required to make quantitative determinations of hadronic effects. Of these *Lattice QCD*, i.e. the use of lattice formulations of QCD in large scale numerical simulations has emerged in recent years as a precise *ab initio* technique which can be applied to a wide range of processes and physical quantities.

As the name suggests, the evaluation of hadronic effects in lattice QCD is performed by approximating space–time by a discrete lattice of points in each space–time direction in Euclidean space. A schematic sketch is shown in Fig. 1(a).

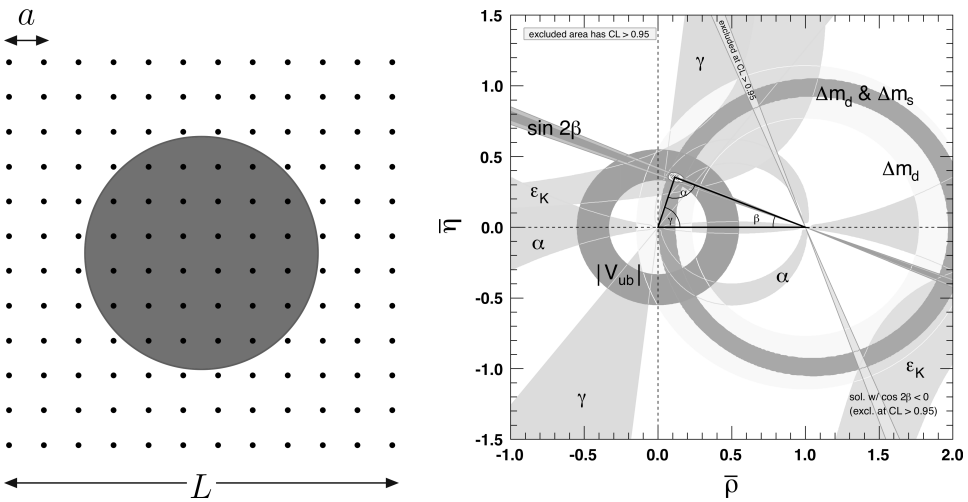

(a) (b)

Fig. 1. (a) Schematic illustration of a Euclidean lattice where a represents the lattice spacing and L its spacial extent. The green circle represents the hadron which is being studied. (b) Determination of the vertex $(\bar{\rho}, \bar{\eta})$ of the unitarity triangle from a variety of weak decay processes.[42]

The quark fields $\psi(x)$ are placed at the lattice sites, whereas gluon fields $A_\mu(x)$ are introduced in terms of *links* $U_\mu(x) = e^{iA_\mu(x+a\hat{\mu}/2)}$, where a is the spacing between neighbouring points and $\hat{\mu}$ is the unit vector in the μ direction. (Throughout this paper the lattice spacing will be denoted by a.) The links transform covariantly under SU(3) gauge transformations $U_\mu(x) \to g(x)U_\mu(x)g^\dagger(x+\hat{\mu})$ ($\psi(x) \to g(x)\psi(x)$), making it possible to construct lattice QCD actions which are exactly gauge invariant. Here we do not review the different discretisations of QCD which are used in actual simulations, but refer the reader to some of the many excellent textbooks on the subject.[2–5]

The applications of lattice QCD are numerous and it is not possible to review them all here. For example at the most recent annual symposium on lattice field theory[6] there were parallel sessions on hadron spectroscopy and interactions; hadron structure; standard model parameters and renormalisation; physics beyond the standard model; weak decays and matrix elements; QCD at nonzero temperature and density; chiral symmetry; vacuum structure and confinement, as well as on new theoretical developments, on algorithms and machines and on applications beyond QCD. In this review I will focus on some of the applications to particle physics phenomenology in general and to flavour physics in particular (see the chapters by G. Isidori[7] and F. Teubert[8] in this Book). In flavour physics we explore the limits of the standard model and search for signatures of new physics by overdetermining the four parameters of the Cabibbo–Kobayashi–Maskawa (CKM) matrix using numerous different physical processes and checking for inconsistencies. The central role of lattice simulations here is in quantifying the hadronic effects, without which the

CKM elements in general cannot be determined, and several examples are given below. This is illustrated in Fig. 1(b) in which the status of the vertex $(\bar{\rho}, \bar{\eta})$ of the unitarity triangle is shown.[42] Lattice results are used in extracting information about the CKM matrix elements when using the measured values of the indirect CP-violation parameter ϵ_K, the mass differences of neutral B mesons (Δm_d and Δm_s) and the determination of $|V_{ub}|$ from exclusive decays.

Numerical results from lattice simulations are constantly improving and I will not attempt to provide an independent detailed compilation of all the results and uncertainties. The *Flavour Physics Lattice Averaging Group* FLAG, performs detailed critical analyses of the computations and results and so far has published two editions of its reviews with a third one scheduled for early in 2016.[11,12] Throughout this paper I illustrate the discussion by quoting the averages from Ref. 12.

The plan of the remainder of this review is as follows. The following section contains a brief introduction to lattice phenomenology with the aim of providing the non-specialist reader with some intuition as to which quantities are calculable and what the limitations on precision are. In Section 3 I discuss the determination of the parameters of QCD, i.e. the quark masses and the strong coupling constant. This is followed by a discussion of a selection of important quantities in flavour physics, including the leptonic decay constants of pseudoscalar mesons, the B-parameters of neutral meson mixing, semileptonic decays as well as nonleptonic kaon decays whose amplitudes were computed for the first time very recently. Prospects for extending the range of lattice computations in flavour physics are briefly discussed in Section 5 and the review concludes with a brief summary.

2. Introduction to Lattice Phenomenology

Lattice phenomenology starts with the evaluation of correlation functions of the form:

$$\langle 0|\, O(x_1, x_2, \ldots, x_n)\, |0\rangle = \frac{1}{Z} \int [dA_\mu]\, [d\psi]\, [d\bar{\psi}]\, e^{iS}\, O(x_1, x_2, \ldots, x_n), \qquad (1)$$

where $O(x_1, x_2, \ldots, x_n)$ is a multilocal operator composed of quark and gluon fields and Z is the partition function:

$$Z = \int [dA_\mu]\, [d\psi]\, [d\bar{\psi}]\, e^{iS}\ . \qquad (2)$$

In lattice simulations, the infinite-dimensional functional integrals in Eq. (1) are performed by discretising space–time, and using Monte Carlo integration in Euclidean space. The physics which can be studied by computing correlation functions depends on the choice of the multilocal operator O. To illustrate this, consider two-point correlation functions of the form:

$$C_2(t) = \int d^3x\ e^{i\vec{p}\cdot\vec{x}}\ \langle 0|\, \phi_H(\vec{x}, t)\, \phi_H^\dagger(\vec{0}, 0)\, |0\rangle, \qquad (3)$$

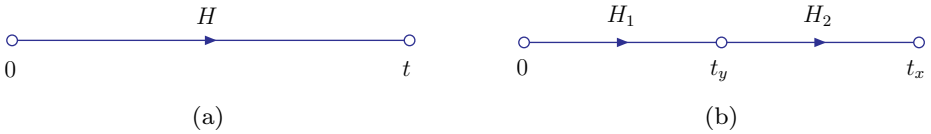

Fig. 2. Schematic illustrations of two- and three-point correlation functions.

where ϕ_H is any interpolating operator for the hadron H whose properties we wish to determine and the time t is taken to be positive. We assume that H is the lightest hadron which can be created by $\phi_H^\dagger$ and that $t > 0$. Inserting a complete set of states between the operators in Eq. (3) and exploiting translational invariance one obtains for sufficiently large t in Euclidean space

$$C_2(t) = \frac{1}{2E_H}\, e^{-E_H t}\, |\langle 0|\phi_H(0)|H(p)\rangle|^2 + \cdots , \tag{4}$$

where $E_H = \sqrt{m_H^2 + \vec{p}^{\,2}}$. A schematic sketch of $C_2(t)$ is shown in Fig. 2(a). The ellipsis in Eq. (4) represents contributions from heavier states with the same quantum numbers as H and which fall more rapidly with t. By fitting $C_2(t)$ as a function of t (at sufficiently large t so that the excited states in Eq. (4) can be neglected) we obtain both the mass m_H and the matrix element $|\langle 0|\phi_H(0)|H(p)\rangle|$. For example, if ϕ_H is the axial current $\bar{q}_1\gamma^\mu\gamma^5 q_2$, where $q_{1,2}$ are the valence quarks of the pseudoscalar meson P, then we obtain the leptonic decay constant f_P as discussed in Section 4.1.

To obtain matrix elements of the form $\langle H_2 \,|\, O \,|\, H_1\rangle$, where $H_{1,2}$ are single-hadron states and O is a composite operator of quark and gluon fields, we evaluate three-point correlation functions of the form

$$C_3(t_x, t_y) = \int d^3x\, d^3y\; e^{i\vec{p}\cdot\vec{x}}\; e^{i\vec{q}\cdot\vec{y}}\; \langle 0|\phi_{H_2}(\vec{x}, t_x) O(\vec{y}, t_y)\phi^\dagger_{H_1}(\vec{0}, 0)|0\rangle \tag{5}$$

$$= \frac{e^{-E_{H_1} t_y} e^{-E_{H_2}(t_x - t_y)}}{(2E_{H_1})(2E_{H_2})} \langle 0|\phi_{H_2}(0)|H_2(\vec{p})\rangle$$

$$\times \langle H_2(\vec{p})|O(0)|H_1(\vec{p}+\vec{q})\rangle \langle H_1(\vec{p}+\vec{q})|\phi^\dagger_{H_1}(0)|0\rangle, \tag{6}$$

where ϕ_{H_1,H_2} are interpolating operators for H_1, H_2 and we assume that $t_x > t_y > 0$. All the factors in (6) can be obtained from two-point functions as described above with the exception of the matrix element $\langle H_2(\vec{p})|O(0)|H_1(\vec{p}+\vec{q})\rangle$ which is therefore determined from the computation of the three-point functions. In this way we can obtain for example, weak and electromagnetic form factors, the amplitudes for neutral meson mixing (such as the B_K parameter of $K-\bar{K}$ mixing) and the moments of hadronic structure functions.

By computing correlation functions of the form C_2 and C_3, the determination of the spectrum and of matrix elements of local operators O between single hadron states is now standard. We briefly discuss the status of the (non-standard as yet)

evaluation of matrix elements with multi-hadron states and of non-local operators below.

2.1. *Uncertainties in lattice simulations*

Before presenting results, I briefly discuss some of the main contributions to the uncertainties. The evaluation of the correlation functions C_2 and C_3 is performed using Monte Carlo sampling and has an associated statistical error which is estimated by observing how the results vary as additional field configurations are added or removed. More problematic is a reliable determination of the systematic uncertainties. Some of these are specific to the particular quantities being computed; here I mention those which are common to most computations.

2.1.1. *Unphysical light-quark masses*

For much of the period since the 1980's, when lattice computations were in their infancy, the simulations were performed in the *quenched* approximation in which vacuum polarisation effects (sea-quark loops) are neglected. In practice this is implemented by setting the fermionic determinant $\mathrm{Det}(D[A]) = 1$, where $D[A]$ is the Dirac operator in the presence of the background gluon field configuration $\{A(x)\}$. This determinant arises from the integration over the quark fields in Eqs. (1) and (2); it is non-local and its presence makes the generation of the gluon configurations significantly more expensive. Whilst results for known quantities were typically correct at the 10–20% level, the problem with the quenched approximation is that the associated errors cannot be reliably determined.

From around 2000, unquenched simulations became possible albeit with unphysically heavy u- and d-quark masses m_u and m_d; generally the corresponding pion masses were in the range of 0.5–1 GeV. To obtain physical quantities it was therefore necessary to extrapolate in the light-quark masses, frequently using chiral perturbation theory (ChPT) to guide the extrapolation. Indeed as the quark masses were reduced the lattice simulations provided tests of the range of applicability of ChPT and a determination of the corresponding low-energy constants.[13,14] Today we are in the early years of simulations performed with physical values of m_u and m_d (or at least their average $(m_u + m_d)/2$). The next challenge is to include and control isospin breaking effects (including electromagnetic effects). An interesting recent example is the determination of the neutron–proton mass difference by the BMW collaboration.[9] For electromagnetic corrections to amplitudes, one has to control the cancelation of infrared divergences and some initial thoughts were presented earlier this year.[10]

2.1.2. *Lattice spacings and volumes*

Since the cost of the simulations is largely proportional to the number of points in each direction, the choice of the lattice spacing is a compromise between the two

conflicting requirements of a fine lattice to minimise lattice artefacts (discretisation errors) and simultaneously one with a large physical volume. At present, depending on the discretisation of QCD being used and on the values of the light quark masses, typical values of the lattice spacing are in the range $0.05-0.1$ fm and typical volumes are of the order of a few fm, perhaps 5 fm or so. A natural approach to quantifying the errors due to the finite lattice spacing a and volume V is to perform several simulations at different values of a and V and to perform the extrapolations to the continuum and infinite-volume limits and indeed this is done in many cases. In addition one can choose an *improved* discretisation of QCD in which the lattice artefacts decrease as higher powers of a. For example, the artefacts in results obtained using the original Wilson formulation of lattice fermions fall linearly with a whereas with many other formulations they decrease quadratically. The finite-volume corrections are dominated by the propagation of the lightest particles, the pseudo-Goldstone bosons of chiral symmetry breaking (pions and kaons) and so ChPT can be used to estimate these effects. In a finite volume the momentum spectrum is discrete and so infinite-volume momentum integrals are replaced by finite-volume sums and the Poisson summation formula is a powerful tool for calculating the difference between the two.

2.2. *Renormalisation*

A lattice formulation of QCD can be considered as a bare quantum field theory with a playing the role of the ultraviolet cut-off. Quantities computed directly in lattice simulations therefore generally require renormalisation. These might be the QCD parameters (see Section 3) or composite operators which appear when describing physical quantities using the Operator Product Expansion (OPE). With $a^{-1} \leq 4$ GeV it is not possible to simulate the entire standard model and so we have to rely on the OPE and effective theories, writing physical quantities ϕ in the schematic form:

$$\phi = \sum_i C_i(\mu^2) \langle f | O_i^{\rm R}(\mu^2) | i \rangle, \tag{7}$$

where the $O_i^{\rm R}(\mu^2)$ are renormalised composite local operators and μ^2 is the renormalisation scale. $|i\rangle$ and $|f\rangle$ denote the initial and final states respectively. The long-distance non-perturbative physics is contained in the operator matrix elements. The Wilson coefficients $C_i(\mu^2)$ contain the short-distance physics and are calculated in perturbation theory, generally in the $\overline{\rm MS}$ scheme which is convenient for perturbative calculations.

In lattice simulations we compute directly the matrix elements of the bare operators $O_i^B(a)$ in the discretisation of QCD which is being used. For sufficiently large ultraviolet cut-off a^{-1} and renormalisation scale μ it is possible to relate the bare and renormalised operators using perturbation theory and this was done in the early days of lattice QCD. Calculating higher order perturbative calculations

in lattice QCD is challenging however, and frequently leads to large corrections. It is now common practice instead to impose the renormalisation conditions non-perturbatively.[15,16] In this way the renormalisation matrix $Z_{ij}(\mu a)$ relating the bare and renormalised operators,

$$O_i^R(\mu^2) = \sum_j Z_{ij}(\mu a)\, O_j^B(a), \tag{8}$$

is determined numerically and often with excellent precision. Some element of perturbation theory is needed however, since the perturbative calculations of the Wilson coefficients C_i are generally performed in schemes based on dimensional regularisation (such as $\overline{\rm MS}$) which cannot be simulated. A continuum perturbative calculation is therefore needed to relate the operators renormalised in a scheme which can be imposed in a lattice simulation and that used in the calculation of the Wilson coefficients.

2.3. *Heavy quarks*

Weak decays of charm and bottom hadrons provide a particularly rich source of information with which to perform precision studies in flavour physics. They are sufficiently light to be produced copiously and yet heavy enough to have a huge number of possible decay channels, many of which are very rare within the standard model and which can therefore be used to search for evidence of new physics. It appears that the lattice spacings currently being used are sufficiently fine for the charm quark to be simulated using a discrete version of the corresponding terms in the QCD action, but for the b-quark $m_b a > 1$ and such simulations are inappropriate. Most approaches to B-physics rely on effective theories which then have to be matched to QCD. The most common ones use (i) the Heavy Quark Effective Theory which is an expansion in $\Lambda_{\rm QCD}/m_B$ (see Ref. 17 for a recent review), (ii) nonrelativistic QCD which is an expansion in the heavy quark's velocity[18,19] and (iii) the relativistic heavy quarks approach of the Fermilab group[20] and its extensions.[21] Some groups also extrapolate results from the charm to the bottom region, using scaling laws where applicable and possibly using results in the static limit in which the heavy quark is treated as being infinitely heavy. There are far fewer calculations in heavy-quark physics than of light-quark quantities (although this is currently changing) and so there has been less opportunity to check for consistency of the different approaches.

3. Determination of α_s and the Quark Masses

The strong coupling α_s and the quark masses are input parameters into QCD. They are not measurable directly, but have to be inferred from their effect on measurable quantities such as hadronic masses or, as we shall see below, on other quantities which can be computed in lattice simulations.

To illustrate the procedure consider simulations with $N_f = 2 + 1$ flavours, i.e. with a sea of u, d, s quarks with $m_u = m_d$. This is a typical situation, although increasingly charm quarks are also introduced into the sea. In each simulation numerical values of the bare strong coupling constant $g(a)$ and the bare quark masses are entered into the computation. If computing resources were unlimited, we would vary the bare quark masses until two dimensionless quantities agreed with their physical values; e.g. a popular choice is m_π/m_K and m_π/m_Ω. Given that the input bare quark masses are chose *a priori* and that resources are in fact limited, such a procedure is adapted to include extrapolations or interpolations of results obtained from several simulations and/or with the use of ChPT. To determine the lattice spacing a, we take the lattice result for a dimensionful quantity obtained in "lattice units", e.g. am_Ω, and write

$$a^{-1} = \frac{1.672\,\text{GeV}}{(am_\Omega)}, \tag{9}$$

where the physical value of $m_\Omega = 1.672\,\text{GeV}$. Having determined the bare quark masses $m_f(a)$, where f denotes the flavour, we need to renormalise them into a standard scheme, such as the $\overline{\text{MS}}$ scheme. For the light-quark masses the FLAG collaboration[12] quotes from $N_f = 2+1$ simulations, $m_{ud}^{\overline{\text{MS}}}(2\,\text{GeV}) = 3.42(6)(7)\,\text{MeV}$ and $m_s^{\overline{\text{MS}}}(2\,\text{GeV}) = 93.8(1.5)(1.9)\,\text{MeV}$.

In order to obtain m_u and m_d separately, rather than just their average, isospin breaking effects must be included and this is beginning to be done. In the meantime the FLAG results shown in Table 1 combine additional ChPT/Current Algebra phenomenological input with lattice results obtained from isospin-symmetric computations.

The traditional determination of the strong coupling constant α_s without using lattice QCD inputs relies on comparing experimental results for some short distance quantities (such as hadronic τ decays, $e^+e^- \to$ hadrons, deep inelastic lepton-hadron scattering and electroweak precision measurements) with the corresponding perturbative expansion. This is reviewed by G. Dissertori in this Book.[22] The PDG[42] quote $\alpha_S^{(5)}(M_Z) = 0.1183 \pm 0.0012$ for the $\overline{\text{MS}}$ coupling in the 5-flavour theory renormalised at M_Z obtained without using lattice inputs. The use of lattice simulations has the advantage that the short-distance quantities do not have to be physically measurable. The procedure is therefore to determine such a quantity ϕ^{SD} nonperturbatively in a lattice computation and to compare the result with the perturbation series:

$$\phi^{\text{SD}} = \sum_i c_i(\mu)\, \alpha_S^i(\mu) + \cdots, \tag{10}$$

where SD reminds us that the quantity must be a short-distance one and the ellipsis represents power corrections which are sometimes modelled and included in the fits. Choices for ϕ^{SD} include the heavy-quark potential, the correlation functions C_2 evaluated at short-distances or large momenta, small loops composed of products of

Table 1. Results taken from the summary table from the FLAG compilation,[12] grouped in terms of N_f, the number of dynamical quark flavours in lattice simulations. The quark masses are given in the $\overline{\text{MS}}$ scheme at running scale $\mu = 2\,\text{GeV}$. The columns marked ■ indicate the number of results that enter the averages for each quantity having satisfied the quality criteria. Full details of the analyses for each quantity can be found in the corresponding sections of Ref. 12. The f_P are the leptonic decay constants of the pseudoscalar meson P (normalised so that $f_\pi \simeq 131\,\text{MeV}$), the $\hat{}$ denotes the renormalisation group invariant definition of the B-parameters and $\xi = f_{B_s}\sqrt{B_{B_s}}/f_{B_d}\sqrt{B_{B_d}}$.

Quantity	■	$N_f = 2+1+1$	■	$N_f = 2+1$	■	$N_f = 2$
m_s(MeV)			3	93.8(1.5)(1.9)	2	101(3)
m_{ud}(MeV)			3	3.42(6)(7)	1	3.6(2)
m_s/m_{ud}			3	27.46(15)(41)	1	28.1(1.2)
m_d(MeV)				4.68(14)(7)		4.80(23)
m_u(MeV)				2.16(9)(7)		2.40(23)
m_u/m_d				0.46(2)(2)		0.50(4)
$f_+^{K\pi}(0)$			2	0.9661(32)	1	0.9560(57)(62)
f_{K^+}/f_{π^+}	2	1.194(5)	4	1.192(5)	1	1.205(6)(17)
f_K(MeV)			3	156.3(0.9)	1	158.1(2.5)
f_π(MeV)			3	130.2(1.4)		
$\hat{B}_K$			4	0.766(10)	1	0.729(25)(17)
$B_K^{\overline{\text{MS}}}(2\,\text{GeV})$			4	0.560(7)	1	0.533(18)(12)
f_D(MeV)			2	209.2(3.3)	1	208(7)
f_{D_s}(MeV)			2	248.6(2.7)	1	250(7)
f_{D_s}/f_D			2	1.187(12)	1	1.20(2)
$f_+^{D\pi}(0)$			1	0.666(29)		
$f_+^{DK}(0)$			1	0.747(19)		
f_B(MeV)	1	186(4)	3	190.5(4.2)	1	189(8)
f_{B_s}(MeV)	1	224(5)	3	227.7(4.5)	1	228(8)
f_{B_s}/f_B	1	1.205(7)	2	1.202(22)	1	1.206(24)
$f_{B_d}\sqrt{\hat{B}_{B_d}}$(MeV)			1	216(15)		
$f_{B_s}\sqrt{\hat{B}_{B_s}}$(MeV)			1	266(18)		
$\hat{B}_{B_d}$			1	1.27(10)		
$\hat{B}_{B_s}$			1	1.33(6)		
ξ			1	1.268(63)		
$\hat{B}_{B_s}/\hat{B}_{B_d}$			1	1.06(11)		
$\alpha_{\overline{\text{MS}}}^{(5)}(M_Z)$			4	0.1184(12)		

gauge links, as well as quark–gluon vertices at large external momenta. Although the perturbative coefficients are frequently known to impressive orders of perturbation theory, the unavoidable truncation of the series in Eq. (10) is one of the main sources of systematic error. A related limitation is the size of the typical lattice spacing $a^{-1} \simeq 2{-}4\,\text{GeV}$ at which the coupling constant is still fairly large. This can be overcome in principle, and increasingly frequently in practice, by the use of *step scaling*. While lattices on which hadrons are studied necessarily have spacial extents of a least a few fermi, this is not the case for the short-distance quantities

used in determining α_S, or in performing renormalisation in general. Step scaling is the successive matching of one lattice with a finer one until we end up with a lattice with a sufficiently small lattice spacing allowing for a reliable perturbation series. The FLAG collaboration have critically reviewed the current lattice determinations of α_S and (conservatively) quote

$$\alpha_S^{(5)}(M_Z) = 0.1184 \pm 0.0012, \tag{11}$$

as their combined result. It should be noted that the result in (11) has a larger uncertainty than those quoted in several of the publications analysed in arriving at this result; the reasons for this are explained in Ref. 12.

4. Selected Quantities in Flavour Physics

It is not possible in this brief review to discuss every physical quantity and to analyse every lattice computation. For many quantities in flavour physics this task has been undertaken by the FLAG collaboration.[12] I will comment on a number of the quantities studied by FLAG, but start this section by reproducing in Table 1 part of the summary table of Ref. 12. The reader who is interested in specific quantities will find a critical analysis of each computation and references to the original literature in Ref. 12.

4.1. *Leptonic decays of mesons*

Among the simplest quantities for which the nonperturbative QCD effects can be computed are the amplitudes for the leptonic decays $P^+ \to \ell^+\nu_\ell$ where P is a pseudoscalar meson and ℓ a lepton. Lorentz and parity symmetries imply that all the hadronic effects are contained in a single *decay constant*, f_P, defined by:

$$\langle 0|\, \bar{q}_2\gamma_\mu\gamma_5 q_1\, |P^+\rangle = i f_P p_\mu\,, \tag{12}$$

where q_1 and q_2 are the charge $2/3$ and $-1/3$ valence quark fields of P^+ respectively. In terms of f_P the decay rate is written as

$$\Gamma(P^- \to \ell^-\bar{\nu}_\ell) = \frac{G_F^2\,|V_{q_1q_2}|^2 f_P^2}{8\pi}\, m_P\, m_\ell^2 \left(1 - \frac{m_\ell^2}{m_P^2}\right)^2 . \tag{13}$$

The decay constants are obtained from a calculation of two-point correlation functions with suitable interpolating operators for the mesons. A recent compilation of the results is presented in Table 1,[12] from which I wish to make two points. The first is to underline the remarkable progress in lattice calculations, which can be seen in the very small errors, approaching 1% precision or even better. Secondly, if the improved precision is to be reflected in an improved determination of the CKM matrix elements $V_{q_1q_2}$ isospin breaking effects, including electromagnetic corrections must be included.[10,28]

4.2. *Neutral-meson mixing and semileptonic decays of pseudoscalar mesons*

We have seen that from three-point correlation functions we can obtain matrix elements of the form $\langle f|O(0)|i\rangle$ where $O(0)$ is a local composite operator. As illustrations of the physics which can be studied this way, we will consider the mixing of neutral pseudoscalar mesons $P^0 \leftrightarrow \bar{P}^0$ and the semileptonic decays $P_1 \to P_2 \ell \nu_\ell$, where $P_{1,2}$ are pseudoscalar mesons and ℓ is a lepton.

Figure 3(a) shows the quark-flow diagram for neutral kaon mixing. In the standard model, the non-perturbative hadronic effects in the dominant contribution to the indirect CP-violation parameter ϵ_K are contained in the matrix element of a single $\Delta S = 2$ four-quark operator

$$\langle \bar{K}^0 | \left(\bar{s}\gamma^\mu(1-\gamma^5)d\right)\left(\bar{s}\gamma_\mu(1-\gamma^5)d\right)|K^0\rangle \equiv \frac{8}{3} f_K^2 B_K(\mu)\,, \tag{14}$$

where f_K is the leptonic decay constant of the kaon and it is conventional to parametrise the matrix element in terms of B_K. μ represents the scale at which the operator has been renormalised. A summary of the lattice results for B_K and the corresponding quantities B_{B_d} and B_{B_s} for B-meson mixing is given in Table 1. The impressive precision of these results is now such that subdominant contributions need also to be evaluated and in Sec. 5.2 I briefly discuss the prospects for the evaluation of the long-distance contributions to ϵ_K which are expected to be $O(5\%)$.

Another important class of quantities which can be obtained from the evaluation of three-point functions are electromagnetic and weak form factors of both mesons and baryons. Within flavour physics, lattice evaluations of the weak transition form factors combined with experimental measurements of the decays rates are used to determine the corresponding CKM matrix elements. Here we illustrate this by considering semileptonic $B \to \pi \ell \nu_\ell$ decays from which the CKM matrix element V_{ub} can be determined. As is frequently the case, the main limitation on the precision in the determination of V_{ub} is due to that with which we can compute the hadronic effects. These are contained in two invariant form factors $f_{0,+}$

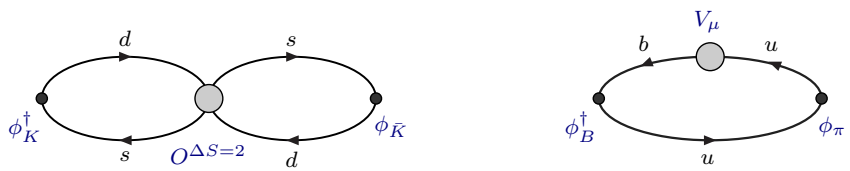

Fig. 3. Schematic illustrations of the correlation functions from which the B_K parameter of K^0–$\bar{K}^0$ mixing and the semileptonic $B \to \pi$ form-factors are obtained.

defined by

$$\langle \pi(p_\pi)|\bar{b}\gamma^\mu u|B(p_B)\rangle = f_0(q^2)\frac{m_B^2 - m_\pi^2}{q^2} + f_+(q^2)\left[(p_\pi + p_B)_\mu - \frac{m_B^2 - m_\pi^2}{q^2}q_\mu\right], \tag{15}$$

where $q = p_B - p_\pi$. The form factors are obtained from the computation of the three-point function in (5) with $\phi^\dagger_{H_1} = \phi^\dagger_B$, an interpolating operator with the quantum numbers to create a B-meson, $O(\vec{y}, t_y) = V_\mu(\vec{y}, t_y)$ the $b \to u$ weak vector current and $\phi_{H_2} = \phi_\pi$ an interpolating operator which can annihilate the pion. The evaluation of such form factors can readily be generalised to other pseudoscalar mesons in the initial and final states and extended to form factors of other operators and particles (e.g. to vector particles as in $B \to \rho$ semileptonic decays). In the case of $B \to \pi\ell\nu_\ell$ decays, for much of the phase space the pions have momenta which are large enough to resolve the discrete nature of the lattice. The calculations are therefore restricted to small pion momenta, which corresponds to large values of q^2. V_{ub} is obtained by combining the lattice results with a subset of the experimental data:

$$\Delta\zeta(q_1^2, q_2^2) \equiv \frac{1}{|V_{ub}|^2}\int_{q_1^2}^{q_2^2} dq^2\ \frac{d\Gamma}{dq^2}.$$

(The lattice results at large q^2 can also be combined with theoretically motivated parametrisations for the form factors at lower q^2, including perhaps constraints from analyticity and other general properties of field theory, to extend the range of the predictions, but this is not discussed here.) The two longstanding results for the form-factors are from the FNAL/MILC[23] and HPQCD collaborations[24] are these are combined in the FLAG compilation to give[12]

$$\Delta\zeta(16\,\mathrm{GeV}^2, q^2_{\mathrm{max}}) = 2.16(50)\,\mathrm{ps}^{-1}\,. \tag{16}$$

Combining this result with the experimental data from the BaBar (Belle) experiments, the FLAG collaboration find $V_{ub} = 3.37(21) \times 10^{-3}$ $(3.47(22) \times 10^{-3})$.[12] There is an interesting tension between results such as these obtained from exclusive decays and those obtained from inclusive $b \to u$ semileptonic decays,[42] $|V_{ub}| = (4.41 \pm 0.15^{+0.15}_{-0.19}) \times 10^{-3}$. The determination from inclusive decays has very different systematics and cannot be studied in lattice simulations. The evaluation of $f_+(q^2)$ and $f_0(q^2)$ and the subsequent determination of V_{ub} is a major priority for several collaborations (see e.g. Refs. 25 and 29 for two recent studies).

Until this year, the exclusive determination of V_{ub} has been largely performed by studying B-meson decays. A very interesting recent development has been the determination by the LHCb collaboration of $V_{ub} = (3.27 \pm 0.23) \times 10^{-3}$ from the baryonic decay $\Lambda_b^0 \to p\mu^-\bar{\nu}_\mu$[26] using form factors computed in lattice simulations.[27]

4.3. *Hadronic decays*

Up to now we have considered matrix elements of the form $\langle f|O(0)|i\rangle$ where $|i\rangle$ and $|f\rangle$ are single-particle states or the vacuum. Much of standard model phenomenology, whether involving decays or scattering, concerns multi-hadron states and it turns out that these are considerably harder to deal with in Euclidean finite-volume computations. Before studying the decays however, consider the propagation of a two-pion state with energy below the inelastic threshold. In a series of pioneering papers Lüscher showed how the corresponding energy levels depend on the finite volume and that they are given in terms of the physical scattering $\pi\pi$ phase-shifts.[30–32] For example, assuming that the s-wave $\pi\pi$ scattering is dominant, the Lüscher quantisation condition for the (discrete) two-pion energies in a finite-volume ($E_{\pi\pi}$) takes the form $\phi(p^*) + \delta_s(p^*) = n\pi$ where n is an integer, the relative momentum $p^* = \frac{1}{2}\sqrt{E_{\pi\pi}^2 - 4m_\pi^2}$, ϕ is a known kinematic function and δ_s is the s-wave phase-shift in the appropriate isospin channel. The quantisation condition can be generalised to include higher partial waves. This remarkable formula allows for a determination of the elastic scattering phase-shifts from the measured two-pion energy levels in a finite Euclidean volume. The formalism applies also to other two-body systems, including pion–nucleon states below the inelastic threshold.

The generalisation to states with higher multiplicities is much more difficult and so far has been restricted to theoretical studies of three-particle states with the recent completion of a formalism to relate the finite-volume three-body spectrum to the three-to-three scattering amplitude for a scalar quantum field theory.[33]

4.3.1. *Two-body decay amplitudes*

The finite-volume approach has been extended to the study of two-body decays. A particularly important example is that of nonleptonic $K \to \pi\pi$ decays in which both indirect and direct CP-violation were first discovered. Bose symmetry implies that the total isospin I of the final two-pion state is either 0 or 2. The evaluation of the $K \to \pi\pi_{I=2}$ amplitude A_2 has recently been achieved with physical kaon and pion masses.[34–36] Whereas for single-hadron states the finite-volume corrections decrease exponentially with the volume, for two-hadron states they only fall as powers of the volume. These effects are also given in terms of the phase-shifts (or more precisely of the derivatives of the phase-shifts with respect to the centre-of-mass momentum) and can be corrected by a multiplicative factor, the *Lellouch–Lüscher factor*.[38–40]

The evaluation of the $K \to (\pi\pi)_{I=0}$ amplitude A_0 is much more involved and complicated and it has only been very recently that the first calculation, performed with physical masses and kinematics, has been completed.[41] The evaluation of the $K \to \pi\pi$ amplitudes, in particular A_0, has for several decades been a seemingly unattainable target for lattice computations. It is therefore particularly satisfying

that this target has now been reached, albeit still with significant uncertainties[41]:

$$\mathrm{Re}\left(\frac{\epsilon'}{\epsilon}\right) = (1.38 \pm 5.15 \pm 4.43) \times 10^{-4}, \tag{17}$$

where the first error is statistical and the second is systematic. The Particle Data Group compilation[42] of the experimental results is $\mathrm{Re}(\epsilon'/\epsilon) = 1.66(0.23) \times 10^{-3}$. The matrix elements which contribute to the amplitudes are obtained with better relative accuracy but, as expected, there is a significant partial cancellation between the QCD penguin contribution to $\mathrm{Im}(A_0)/\mathrm{Re}(A_0)$ and the electroweak penguin contribution to $\mathrm{Im}(A_2)/\mathrm{Re}(A_2)$ which amplifies the relative error in $\mathrm{Re}(\epsilon'/\epsilon)$.

4.3.2. *On the difficulty of studying exclusive nonleptonic B decays*

So far in this review we have discussed some of the many physical quantities which can be studied using lattice simulations. It is instructive to examine the main difficulties in the evaluation of $K \to \pi\pi$ amplitudes, because they underline why the calculations cannot be extended to a very important set of processes, two-body B-decays. A huge amount of data has been provided by the B-factories and is being provided by the LHCb experiment on decay rates and CP-asymmetries of processes such as $B \to \pi\pi$ and $B \to \pi K$ and yet without new ideas we cannot compute the corresponding hadronic effects and hence to use this data in studies of the unitarity triangle.

We start the discussion by considering the evaluation of the amplitude A_2 of $K \to (\pi\pi)_{I=2}$ decays illustrated in Fig. 4. We envisage creating a kaon by placing an interpolating operator $\phi_K^\dagger$ at time $t = t_K$ and taking a Fourier transform to project to $\vec{p}_K = 0$. The operators of the strangeness-changing $\Delta S = 1$ effective weak Hamiltonian are placed at t_H, with $t_H - t_K$ sufficiently large to suppress the propagation of states heavier than the kaon between t_K and t_H. By integrating the position of the operators over space, we ensure that the final state also has zero three momentum. Finally at time $t = t_\pi$ we place an operator which can annihilate the two pions. A natural choice for the two-pion interpolating operator is a product of two single-pion annihilation operators, one with momentum $\vec{q}$ and the other with momentum $-\vec{q}$ (see Fig. 4). Among the difficulties in the calculation is that by using

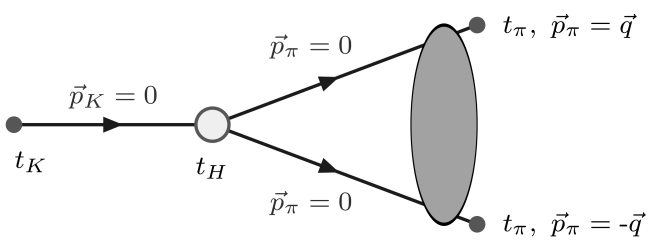

Fig. 4. Schematic illustrations of the correlation functions from which the $K \to (\pi\pi)_{I=2}$ decay amplitude A_2 (see text).

time to isolate the lightest state, energy is not conserved and so $E_{\pi\pi} \neq m_K$ unless we engineer this very carefully. The correlation function sketched in Fig. 4 can be written schematically as a function of $t_\pi - t_H$ in the form:

$$C = C_0 e^{-E^0_{\pi\pi}(t_\pi - t_H)} + C_1 e^{-E^1_{\pi\pi}(t_\pi - t_H)} + \cdots , \tag{18}$$

where $E^0_{\pi\pi}$ and $E^1_{\pi\pi}$ are the energies of the two-pion ground state and first excited state respectively corresponding to the finite volume and boundary conditions used in the simulation. The ellipsis represents the contributions of excited states with energies greater than $E^1_{\pi\pi}$. The lack of energy conservation means that even if the input momentum $\vec{q} \neq 0$, C is dominated by the term with the lowest energy, $E^0_{\pi\pi} = 2m_\pi$ (up to finite volume corrections). The grey oval in Fig. 4 represents the energy non-conserving $\pi\pi$ scattering from $E^0_{\pi\pi}$ to an excited state. In the discussion so far we have implicitly assumed the use of periodic boundary conditions. In such simulations the determination of the physical $K \to \pi\pi$ amplitude requires the study of an excited state with the volume chosen such that $E^1_{\pi\pi} = m_K$ and the determination of C_1; this is very difficult indeed. In the recent computations of A_2, antiperiodic boundary conditions were used instead and the volume was chosen such that the ground state has energy equal to m_K.[34–36]

The s-wave two-pion state $|(\pi\pi)_{I=0}\rangle$ has vacuum quantum numbers and so in addition to the terms on the right-hand side of Eq. (18) there is a constant term corresponding to the vacuum intermediate state which does not fall with $t_\pi - t_H$ and which therefore dominates the correlation function. This complication is unavoidable in the evaluation of A_0 and although the constant is calculable (it is the product of two vacuum expectation values of the form in Eq. (1)) the subtraction of the dominant term leads to a loss of precision. In addition of course, we would like the lowest-energy two-pion state to be the one with $E_{\pi\pi} = m_K$ and this requires the imposition of isospin-conserving G-parity boundary conditions.[43] The vacuum subtraction and the use of G-parity boundary conditions to ensure that the lowest energy of an $I = 0$ two-pion state is m_K were the major technical breakthroughs allowing for the evaluation of ϵ'/ϵ.[41]

Apart from the intrinsic importance of evaluating ϵ'/ϵ from first principle, the main reason for this discussion is to explain a significant limitation of lattice computations; our present inability to calculate exclusive nonleptonic decays in general. Imagine trying to evaluate $B \to \pi\pi$ decay amplitudes and consider Fig. 4 but with the kaon replaced by a B-meson. The pions in the final state each have momenta of about 2.6 GeV. In addition to the requirement of a very fine lattice to accommodate such large momenta, a more serious difficulty is that this corresponds to a highly excited two-pion state with total momentum zero, i.e. one which which is hidden well inside the ellipsis in Eq. (18) and hence is very highly suppressed. One would also need to deal with the power corrections in the volume with many possible intermediate states. Without some novel ideas it is very unlikely that calculations of nonleptonic B and D exclusive decays will be possible in the foreseeable future.

5. New Directions

In the preceding section I described some calculations in flavour physics starting with quantities which can be obtained by computing *standard* two and three-point correlation functions and proceeding to the evaluation of $K \to \pi\pi$ decay amplitudes. In this section I briefly mention some new developments which are likely to extend the physics reach of lattice phenomenology.

5.1. *Hadronic effects in the muon's electric dipole moment*

There is an intriguing 3–4σ discrepancy between the experimental measurement of the anomalous magnetic moment of the muon

$$a_\mu^{\rm exp} = (11659208.9 \pm 6.3) \times 10^{-10} \tag{19}$$

and the standard model prediction

$$a_\mu^{\rm SM} = (11659180.1 \pm 4.9) \times 10^{-10}, \tag{20}$$

(see for example Ref. 44 for a review and references to the original literature). The experimental precision will be significantly improved by new muon $g-2$ experiments at Fermilab and J-PARC. On the theoretical side, in addition to the dominant QED perturbative contributions (and the small weak contributions) there are hadronic effects through the *hadronic vacuum polarisation* (HVP) contribution, estimated using e^+e^- experimental data to be $(682.5 \pm 4.2) \times 10^{-10}$ and the *hadronic light-by-light contribution* (HLbL), estimated using phenomenological techniques to be $(10.5 \pm 2.6) \times 10^{-10}$. It is these hadronic effects, both HVP[45–49] and even HLbL effects[50] which can be estimated using lattice QCD, although it is a challenge to compete with the above precision.

5.2. *Long-distance contributions to hadronic processes*

In Section 4 we have discussed the evaluation of matrix elements of composite local operators. More recently calculations of long-distance effects have begun to

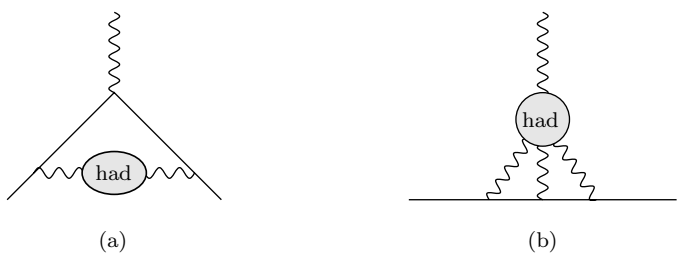

Fig. 5. (a) Hadronic vacuum polarisation and (b) hadronic light-by-light contributions to the anomalous magnetic moment of the muon. The curly lines represent photons and the straight lines the muon.

be evaluated, which involve the determination of non-local matrix elements of the form

$$\int d^4x \int d^4y \langle h_2|T\{O_1(x)O_2(y)\}|h_1\rangle, \tag{21}$$

where $O_{1,2}$ are composite operators and $|\, h_{1,2}\rangle$ are single-hadron states (one can also exploit translational invariance and set either x or y to be the origin for example). An important example is the long-distance contribution to the ϵ_K parameter.[51] This has been estimated to be at the level of a few percent,[52] so since the precision of the hadronic effects in the leading contribution is approaching this level of precision (see the result for B_K in Table 1) it becomes necessary to evaluate the long distance contributions and we can look forward to results in the next few years. Other important quantities for which the long-distance contributions are beginning to be evaluated include the $K_L - K_S$ mass difference[53,54] and rare kaon decays $K \to \pi\nu\bar{\nu}$ and $K \to \pi\ell^+\ell^-$, where ℓ represents a charged lepton.[55,56]

5.3. $R(D)$ and $R(D^*)$

An intriguing tension between experimental observations and standard model predictions is provided by the quantities

$$R(D) = \frac{\mathrm{Br}(\bar{B} \to D\tau^-\bar{\nu}_\tau)}{\mathrm{Br}(\bar{B} \to D\ell^-\bar{\nu}_\ell)} \quad \text{and} \quad R(D^*) = \frac{\mathrm{Br}(\bar{B} \to D^*\tau^-\bar{\nu}_\tau)}{\mathrm{Br}(\bar{B} \to D^*\ell^-\bar{\nu}_\ell)} \tag{22}$$

where $\ell = e$ or μ. Combining the results from Babar[57] and Belle[58] one obtains $R(D) = 0.388 \pm 0.047$ to be compared to the standard model prediction of $R(D) = 0.300 \pm 0.010$. Similarly, combining the Babar, Belle and LHCb[59] results gives $R(D^*) = 0.321 \pm 0.021$ compared to the predicted value of 0.252 ± 0.005. The role of lattice calculations is to evaluate $B \to D^{(*)}$ form factors with good precision. So far this has been done for $B \to D$ form factors with the recent result $R(D) = 0.299 \pm 0.011$[60] and we can anticipate improved precision and also a calculation of $R(D^*)$ in the near future.

6. Summary and Future Prospects

At the 1989 annual symposium on Lattice Field Theory held in Capri, Italy, Ken Wilson the father of the subject, made the prediction that it would take about 30 years before Lattice QCD computations were sufficiently precise and reliable to be useful to Standard Model phenomenology. Although this prediction appeared to be too pessimistic at the time, for much of the intervening period, the systematic uncertainties, and in particular the large values of the u and d sea quark masses in the simulations, meant that extrapolations and model input was necessary to obtain physical results from the computations. This has now changed! Theoretical and algorithmic developments, combined with increased computing resources have led to enormous progress in recent years in the applications of lattice

QCD to Standard Model phenomenology. In this review I have summarised these developments focussing on the determination of the parameters of the standard model and on the applications to precision flavour physics. In the near future, isospin-breaking effects (including electromagnetic corrections) will be included more frequently taking the precision of lattice phenomenology beyond 1%. In addition to continuing to improve the precision of the results for *standard* quantities, the community in also increasing the range of physical quantities and effects which can be studied in lattice simulations. A selection of such extensions was presented in Section 5. We can therefore look forward to an exciting period of time in which new experimental results from the LHC, Belle-II, J-PARC and other facilities are combined with improved lattice computations to explore the limits of the standard model with ever increasing rigour and to help unravel the underlying theoretical framework of the new physics once it is discovered.

References

1. R. K. Ellis, Chapter 3 in this Book.
2. I. Montvay and G. Münster, *Quantum Fields on a Lattice*, Cambridge Monographs on Mathematical Physics (Cambridge University Press, 1994).
3. J. Smit, Cambridge *Lect. Notes Phys.* **15**, 1 (2002).
4. T. DeGrand and C. E. Detar, *Lattice Methods for Quantum Chromodynamics* (World Scientific, 2006).
5. C. Gattringer and C. B. Lang, *Lect. Notes Phys.* **788**, 1 (2010).
6. http://www.aics.riken.jp/sympo/lattice2015/
7. G. Isidori, Chapter 17 in this Book.
8. F. Teubert, Chapter 18 in this Book.
9. S. Borsanyi *et al.*, *Science* **347**, 1452 (2015) [arXiv:1406.4088 [hep-lat]].
10. N. Carrasco, V. Lubicz, G. Martinelli, C. T. Sachrajda, N. Tantalo, C. Tarantino and M. Testa, *Phys. Rev. D* **91**, 7, 074506 (2015) [arXiv:1502.00257 [hep-lat]].
11. G. Colangelo, S. Durr, A. Jüttner, L. Lellouch, H. Leutwyler, V. Lubicz, S. Necco and C. T. Sachrajda *et al.*, *Eur. Phys. J. C* **71**, 1695 (2011) [arXiv:1011.4408 [hep-lat]].
12. S. Aoki, Y. Aoki, C. Bernard, T. Blum, G. Colangelo, M. Della Morte, S. Dürr and A. X. El Khadra *et al.*, *Eur. Phys. J. C* **74**, 2890 (2014) [arXiv:1310.8555 [hep-lat]].
13. S. Dürr *et al.* [Budapest-Marseille-Wuppertal Collaboration], *Phys. Rev. D* **90**, 11, 074506 (2014) [arXiv:1310.3626 [hep-lat]].
14. S. Dürr, PoS LATTICE **2014**, 006 (2015) [arXiv:1412.6434 [hep-lat]].
15. M. Luscher, R. Narayanan, P. Weisz and U. Wolff, *Nucl. Phys. B* **384**, 168 (1992) [hep-lat/9207009].
16. G. Martinelli, C. Pittori, C. T. Sachrajda, M. Testa and A. Vladikas, *Nucl. Phys. B* **445**, 81 (1995) [hep-lat/9411010].
17. R. Sommer, *Nucl. Part. Phys. Proc.* **261–262**, 338 [arXiv:1501.03060 [hep-lat]].
18. B. A. Thacker and G. P. Lepage, *Phys. Rev. D* **43**, 196 (1991).
19. G. P. Lepage, L. Magnea, C. Nakhleh, U. Magnea and K. Hornbostel, *Phys. Rev. D* **46**, 4052 (1992) [hep-lat/9205007].
20. A. X. El-Khadra, A. S. Kronfeld and P. B. Mackenzie, *Phys. Rev. D* **55**, 3933 (1997) [hep-lat/9604004].
21. N. H. Christ, M. Li and H. W. Lin, *Phys. Rev. D* **76**, 074505 (2007) [hep-lat/0608006].

22. G.Dissertori, Chapter 6 in this Book.
23. J. A. Bailey, C. Bernard, C. E. DeTar, M. Di Pierro, A. X. El-Khadra, R. T. Evans, E. D. Freeland and E. Gamiz *et al.*, *Phys. Rev. D* **79**, 054507 (2009) [arXiv:0811.3640 [hep-lat]].
24. E. Dalgic, A. Gray, M. Wingate, C. T. H. Davies, G. P. Lepage and J. Shigemitsu, *Phys. Rev. D* **73**, 074502 (2006) [*Phys. Rev. D* **75**, 119906 (2007)] [hep-lat/0601021].
25. J. A. Bailey *et al.* [Fermilab Lattice and MILC Collaborations], *Phys. Rev. D* **92**, 014024 (2015), arXiv:1503.07839 [hep-lat].
26. R. Aaij *et al.* [LHCb Collaboration], *Nature Phys.* **11**, 743 (2015), arXiv:1504.01568 [hep-ex].
27. W. Detmold, C. Lehner and S. Meinel, *Phys. Rev. D* **92**, 034503 (2015), arXiv:1503.01421 [hep-lat].
28. G. M. de Divitiis *et al.*, *JHEP* **1204**, 124 (2012) [arXiv:1110.6294 [hep-lat]].
29. J. M. Flynn, T. Izubuchi, T. Kawanai, C. Lehner, A. Soni, R. S. Van de Water and O. Witzel, *Phys. Rev. D* **91**, 7, 074510 (2015) [arXiv:1501.05373 [hep-lat]].
30. M. Luscher, *Commun. Math. Phys.* **105**, 153 (1986).
31. M. Luscher, *Nucl. Phys. B* **354**, 531 (1991).
32. M. Luscher, *Nucl. Phys. B* **364**, 237 (1991).
33. M. T. Hansen and S. R. Sharpe, *Phys. Rev. D* **92**, 114509 (2015), arXiv:1504.04248 [hep-lat].
34. T. Blum, P. A. Boyle, N. H. Christ, N. Garron, E. Goode, T. Izubuchi, C. Jung and C. Kelly *et al.*, *Phys. Rev. Lett.* **108**, 141601 (2012) [arXiv:1111.1699 [hep-lat]].
35. T. Blum, P. A. Boyle, N. H. Christ, N. Garron, E. Goode, T. Izubuchi, C. Jung and C. Kelly *et al.*, *Phys. Rev. D* **86**, 074513 (2012) [arXiv:1206.5142 [hep-lat]].
36. T. Blum, P. A. Boyle, N. H. Christ, J. Frison, N. Garron, T. Janowski, C. Jung and C. Kelly *et al.*, *Phys. Rev. D* **91**, 7, 074506 (2015), [arXiv:1502.00263 [hep-lat]].
37. P. A. Boyle *et al.* [RBC and UKQCD Collaborations], *Phys. Rev. Lett.* **110**, 15, 074506 (2013), [arXiv:1212.1474 [hep-lat]].
38. L. Lellouch and M. Luscher, *Commun. Math. Phys.* **219**, 31 (2001) [arXiv:hep-lat/0003023].
39. C. J. D. Lin, G. Martinelli, C. T. Sachrajda and M. Testa, *Nucl. Phys. B* **619**, 467 (2001) [arXiv:hep-lat/0104006].
40. C. h. Kim, C. T. Sachrajda and S. R. Sharpe, *Nucl. Phys. B* **727**, 218 (2005) [hep-lat/0507006].
41. Z. Bai *et al.* [RBC and UKQCD Collaborations], *Phys. Rev. Lett.* **115**, 212001 (2015), arXiv:1505.07863 [hep-lat].
42. K. A. Olive *et al.* [Particle Data Group Collaboration], *Chin. Phys. C* **38**, 090001 (2014).
43. C. Kim and N. H. Christ, PoS LAT **2009**, 255 (2009) [arXiv:0912.2936 [hep-lat]].
44. J. P. Miller, E. d. Rafael, B. L. Roberts and D. Stckinger, *Ann. Rev. Nucl. Part. Sci.* **62**, 237 (2012).
45. C. Aubin and T. Blum, *Phys. Rev. D* **75**, 114502 (2007) [hep-lat/0608011].
46. X. Feng, K. Jansen, M. Petschlies and D. B. Renner, *Phys. Rev. Lett.* **107**, 081802 (2011) [arXiv:1103.4818 [hep-lat]].
47. P. Boyle, L. Del Debbio, E. Kerrane and J. Zanotti, *Phys. Rev. D* **85**, 074504 (2012) [arXiv:1107.1497 [hep-lat]].
48. M. Della Morte, B. Jager, A. Juttner and H. Wittig, *JHEP* **1203**, 055 (2012) [arXiv:1112.2894 [hep-lat]].
49. F. Burger *et al.* [ETM Collaboration], *JHEP* **1402**, 099 (2014) [arXiv:1308.4327 [hep-lat]].

50. T. Blum, S. Chowdhury, M. Hayakawa and T. Izubuchi, *Phys. Rev. Lett.* **114**, 1 (2015), 012001 [arXiv:1407.2923 [hep-lat]].
51. N. Christ *et al.* [RBC and UKQCD Collaborations], PoS LATTICE **2013**, 397 (2014) [arXiv:1402.2577 [hep-lat]].
52. A. J. Buras, D. Guadagnoli and G. Isidori, *Phys. Lett. B* **688**, 309 (2010) [arXiv:1002.3612 [hep-ph]].
53. N. H. Christ *et al.* [RBC and UKQCD Collaborations], *Phys. Rev. D* **88**, 014508 (2013) [arXiv:1212.5931 [hep-lat]].
54. Z. Bai, N. H. Christ, T. Izubuchi, C. T. Sachrajda, A. Soni and J. Yu, *Phys. Rev. Lett.* **113**, 112003 (2014) [arXiv:1406.0916 [hep-lat]].
55. X. Feng, N. H. Christ, A. Portelli and C. Sachrajda, PoS LATTICE **2014**, 367 (2015).
56. N. H. Christ *et al.* [RBC and UKQCD Collaborations], *Phys. Rev. D* **92**, 094512 (2015), arXiv:1507.03094 [hep-lat].
57. J. P. Lees *et al.* [BaBar Collaboration], *Phys. Rev. D* **88**, 7 (2013), 072012 [arXiv:1303.0571 [hep-ex]].
58. A. Bozek *et al.* [Belle Collaboration], *Phys. Rev. D* **82**, 072005 (2010) [arXiv:1005.2302 [hep-ex]].
59. G. Ciezarek, presented on behalf of the LHCb collaboration at the conference *Flavour Physics and CP-violation 2015*, 25–29 May 2015 Nagoya University, Japan.
60. J. A. Bailey *et al.* [MILC Collaboration], *Phys. Rev. D* **92**, 034506 (2015), arXiv:1503.07237 [hep-lat].